ARTICLE

Geometric Design of Anode-Supported Micro-Tubular Solid Oxide Fuel Cells by Multiphysics Simulations

Hong-yu Shi, Jiang Zhu, Zi-jing Lin*

Hefei National Laboratory for Physical Sciences at the Microscale and CAS Key Laboratory of Strongly-Coupled Quantum Matter Physics, Department of Physics, University of Science and Technology of China, Hefei 230026, China

(Dated: Received on April 14, 2017; Accepted on May 19, 2017)

High volumetric power density (VPD) is the basis for the commercial success of micro-tubular solid oxide fuel cells (mtSOFCs). To find maximal VPD (MVPD) for anode-supported mtSOFC (as-mtSOFC), the effects of geometric parameters on VPD are analyzed and the anode thickness, $t_{\rm an}$, and the cathode length, $l_{\rm ca}$, are identified as the key design parameters. Thermo-fluid electrochemical models were built to examine the dependence of the electrical output on the cell parameters. The multiphysics model is validated by reproducing the experimental I-V curves with no adjustable parameters. The optimal $l_{\rm ca}$ and the corresponding MVPDs are then determined by the multiphysics model for 20 combinations of $r_{\rm in}$, the inner tube radius, and $t_{\rm an}$. And all these optimization are made at 1073.15 K. The results show that: (i) significant performance improvement may be achieved by geometry optimization, (ii) the seemingly high MVPD of 11 and 14 W/cm^3 can be easily realized for as-mtSOFC with single- and double-terminal anode current collection, respectively. Moreover, the variation of the area specific power density with $l_{\rm ca}\in$(2 mm, 40 mm) is determined for three representative ($r_{\rm in}$, $t_{\rm an}$) combinations. Besides, it is demonstrated that the current output of mtSOFC with proper geometric parameters is comparable to that of planar SOFC.

Key words: I-V relations, Thermal fluid electrochemistry model, Parametric optimization, Volumetric power density, Anode thickness

I. INTRODUCTION

Due to their high electrical efficiency, fuel flexibility and low pollutant emission, solid oxide fuel cells (SOFCs) bear the promise of revolutionizing the fossil fuel based power generation technology [1]. For applications in the automotive field and in the auxiliary power supply sector, a new design of SOFC, *i.e.*, micro-tubular SOFC (mtSOFC) with a tubular diameter typically under a few millimeters, was developed in 1990s [2]. Since its inception, mtSOFC has shown drastic improvements over the conventional SOFC designs on thermal shock resistance, fast startup and thermal cycling [3]. As a result, mtSOFC is attracting an increased attention in the research and development community [4, 5].

High volumetric power density (VPD) is a prerequisite for the commercial success of mtSOFCs in the field of vehicle applications. To meet the requirements in practice, substantial improvements in the designs of cell geometries, stack configurations, and system operations are required [6]. As mtSOFC is a relatively new design and an mtSOFC cell is the basic electricity generating unit, most research efforts are devoted to the fabrication technique for the performance improvement at the cell level. Like the cases for planar SOFCs (pSOFCs), anode supported mtSOFCs (as-mtSOFCs) show higher performance than their electrolyte- and cathode-supported counterparts. Logically, most researchers focused on as-mtSOFCs for the performance improvement [7−9].

There are a large number of experimental studies on the performances of mtSOFCs with various choices of materials and geometries [4, 10, 11]. Compared with conventional SOFCs, there is hardly anything new about the material choices for mtSOFCs, *e.g.*, YSZ or GDC for the electrolyte, Ni-YSZ or Ni-GDC for the anode, LSCF or LSM for the cathode. However, there are completely new geometric parameters for mtSOFCs, *e.g.*, the tube diameter and length. Moreover, the anode thickness emerges as an influential design parameter as it affects the cell volume and mass that in turn affect the VPD and thermal behavior of mtSOFC. The anode thickness also affects the current collection in most mtSOFC designs that in turn affects the current output of mtSOFC [4]. Furthermore, it has been observed that the cathode location can have substantial influence on the output of mtSOFC [11]. Clearly, attention should be paid to these new geometric parameters when deve-

*Author to whom correspondence should be addressed. E-mail: zjlin@ustc.edu.cn, Tel.: +86-551-63606345, FAX: +86-551-63606348

loping the mtSOFC technology.

There are large differences in the values of anode thickness, tube diameter and cell length of the reported as-mtSOFCs. The anode thickness, though mainly in the range of 200−300 μm, varies from 130 μm [12] to 2 mm [13]. The inner tube diameter is centered around 2 mm, but may vary from 0.8 mm to 22 mm [4]. The cell length varies from a few mm to 160 mm [14−16]. The wide variations in the geometric parameters of the manufactured mtSOFCs may be partly attributed to the difference in the fabrication abilities of different groups. More importantly, the phenomenon reflects the fact that there is no good understanding about the correlation between the geometries and cell performance. Improved understanding is necessary for the realization of the best performing mtSOFCs to make their practical applications a reality. As experimental examination is expensive and time consuming, numerical models incorporating the physics of SOFC to predict the performance are invaluable tools for the understanding and development of mtSOFCs.

In this work, the impact of geometric parameters on VPD of as-mtSOFC was examined by performing systematic multiphysics numerical simulations. The multiphysics model considers the intricate interdependency among the ionic and electronic conductions, gas transport, and electrochemical reaction. The model is validated by comparison with experimental results. Simulations with this validated numerical model provide detailed information about the dependence of VPD on geometric parameters. The optimal geometric parameters and the corresponding power output can be used to guide the design and optimization of as-mtSOFCs.

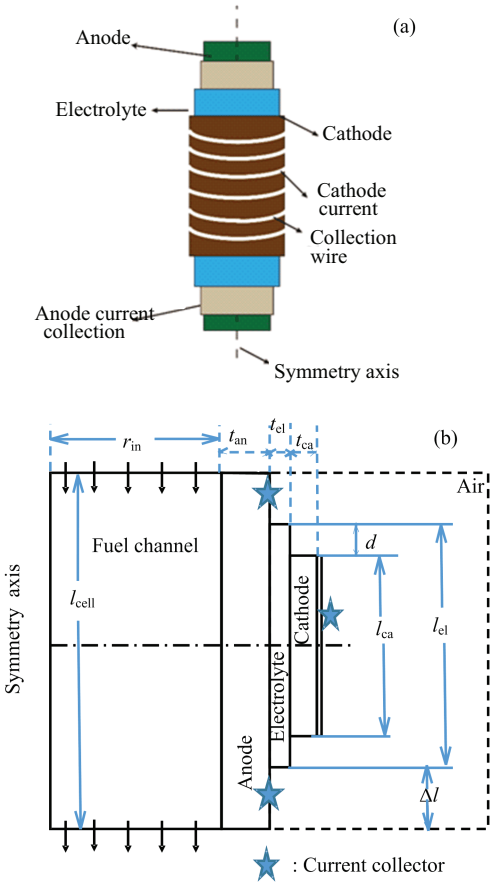

FIG. 1 Schematic diagram of mtSOFC. (a) 3D structure, (b) 2D computational domain.

II. THEORETICAL METHOD

A multiphysics model was built and applied to the geometric model of mtSOFC. Simulations of the multiphysics model are carried out to examine the effect of geometric parameters on the cell output. Optimal geometric parameter sets are determined based on the optimization objective as well as practicality considerations.

A. Geometric model and optimization target

A schematic of an as-mtSOFC is shown in FIG. 1(a). The mtSOFC consists of a porous anode as the inner layer, a dense electrolyte as the middle layer, and a porous cathode as the outer layer. On the cathode side, the current is collected through the cathode surface. On the anode side, the current is collected through the anode current collector(s) at one or both sides of the anode tube. Due to the axial symmetry of mtSOFC, it is necessary only to apply a two-dimensional (2D) geometric model illustrated in FIG. 1(b) for the numerical simulation. The actual 3D structure of the mtSOFC is obtained by revolving the 2D computational domain around the symmetry axis.

The goal of multiphysics simulations is to find the geometric parameters that maximize VPD=$P_{\rm m}/V_{\rm cell}$, where $P_{\rm m}$ and $V_{\rm cell}$ are respectively the maximum electrical power output and the overall volume of the mtSOFC cell. $V_{\rm cell}$ is calculated as,

$$V_{\rm cell} = l_{\rm cell} \cdot \pi r_{\rm out}^2 = \pi l_{\rm cell}(r_{\rm in} + t_{\rm an} + t_{\rm el} + t_{\rm ca})^2 \quad (1)$$

where $l_{\rm cell}$, $r_{\rm out}$, and $r_{\rm in}$ are respectively the length, the outer radius and inner radius of the mtSOFC cell, $t_{\rm an}$, $t_{\rm el}$ and $t_{\rm ca}$ are the thickness of anode, electrolyte and cathode, respectively. The cell length is set as $l_{\rm el}+\Delta l$, where $l_{\rm el}$ is the length of electrolyte and Δl accounts for the required anode current collector, edge sealing, cell connection in a stack, *etc.* The value of Δl is determined by the manufacturing practice. In this work, a value of 6 mm, namely 3 mm for each tube terminal, is used for Δl. Such a value for Δl is believed to be sufficiently large for practical purpose [3]. It is used here also for the purpose of avoiding an overstated maximum VPD (MVPD) achievable by the geometry optimization.

It is reasonable to assume that the current output

DOI:10.1063/1674-0068/30/cjcp1704071

is roughly proportional to the area of electrochemically active region,

$$A_{\rm EC} = 2\pi(r_{\rm in} + t_{\rm an})l_{\rm ca} \tag{2}$$

where $l_{\rm ca}$ is the cathode length (FIG. 1). For a fixed tube radius, the cathode area is proportional to $l_{\rm ca}$. Therefore, it is trivial to expect that MVPD is obtained with the largest possible $l_{\rm ca}$, *i.e.*, $l_{\rm ca}$=$l_{\rm el}$. Though no optimization of $l_{\rm ca}$ is necessary, $l_{\rm ca}$ and the cathode position relative to the anode current collector are variable in the geometric model of FIG. 1(b) so that the simulation results may be compared with the relevant experiments.

Note that the cell volume increases quadratically with $r_{\rm in}$, $t_{\rm an}$, $t_{\rm el}$ and $t_{\rm ca}$, while the electrochemically active area increases linearly with $r_{\rm in}$ and $t_{\rm an}$. This observation calls for as small values of $r_{\rm in}$, $t_{\rm an}$, $t_{\rm el}$ and $t_{\rm ca}$ as possible for obtaining MVPD. In addition, reducing $t_{\rm el}$ also reduces the ohmic polarization. It is then clear that $t_{\rm el}$ should be as small as possible. However, there is a practical lower limit for $t_{\rm el}$ due to the fabrication technique and the required mechanical strength and gas tightness of the electrolyte layer. Though $t_{\rm el}$=1 μm has been reported [17], $t_{\rm el}$ around 5 μm is more manageable in practice [18]. Therefore, a default value of 5 μm is assigned to $t_{\rm el}$, unless explicitly stated otherwise. Similarly, $r_{\rm in}$ cannot be too small due to the fuel supply requirement and the limitation of the fabrication technique. Reducing $t_{\rm ca}$ is also beneficial for the cell performance as long as the cathode layer is adequately thick to accommodate the electrochemical reaction region that is known to be around 10 μm for the widely used cathode materials [19]. Consequently, $t_{\rm ca}$=10 μm is used in this work.

Unlike the cases with $t_{\rm el}$ and $t_{\rm ca}$, reducing $t_{\rm an}$ is detrimental to the anode current collection by reducing the cross section of current passage for the anode current collection method shown in FIG. 1. There should be an optimal balance between the needs of reducing $t_{\rm an}$ for the reduced $V_{\rm cell}$ and increasing $t_{\rm an}$ for the reduction of ohmic polarization. It is noted that the relationship between $t_{\rm an}$ and the current conducting cross section is dependent on the method used for the anode current collection. However, the anode current collection shown in FIG. 1 is widely used for its technical simplicity [3, 4] and is the focus of this study.

A related but different consideration is required for the geometric parameter $l_{\rm el}$=$l_{\rm ca}$. Notice that both the cell volume and the current producing area increase linearly with $l_{\rm el}$=$l_{\rm ca}$. Increasing $l_{\rm el}$=$l_{\rm ca}$ increases the fraction of the current producing area on the cell surface and is beneficial for VPD. However, there is a limit on the total cell current due to the ohmic loss of anode current collection. The cell current production is in fact expected to increase less than linearly with $l_{\rm el}$. As a result, there is an optimal value of $l_{\rm el}$=$l_{\rm ca}$ that yields MVPD.

Based on the above analysis, there are basically two optimizing parameters, $l_{\rm ca}$ and $t_{\rm an}$, for given $r_{\rm in}$ as well as Δl that are set by practical fabrication considerations. Moreover, the anode layer cannot be too thin in an as-mtSOFC. That is, the choice of $t_{\rm an}$ is in fact not arbitrary. Therefore, this work focuses on finding the optimal $l_{\rm cell}$=$l_{\rm ca}$+Δl for a set of practical combinations of $r_{\rm in}$ and $t_{\rm an}$. Nevertheless, the optimal $t_{\rm an}$ for a given $r_{\rm in}$ is also examined.

B. Thermal fluid electrochemistry multiphysics model

A standard set of governing equations for the current-voltage (I-V) relation, mass and momentum transports are applied. The multiphysics equations and the associated source terms used are shown as follows.
For I-V relation:

$$V_{\rm cell} = E_{\rm Nernst} - \eta_{\rm ohm} - \eta_{\rm con} - \eta_{\rm act} \tag{3}$$

For charge transport:

$$\begin{aligned} \nabla\cdot\mathbf{i}_{\rm el} &= \nabla\cdot(-\sigma_{\rm el}\nabla\varphi_{\rm el}) \\ &= \pm j_{\rm TPB}\lambda_{\rm TPB} \qquad \text{(cathode/anode)} \end{aligned} \tag{4}$$

$$\begin{aligned} \nabla\cdot\mathbf{i}_{\rm io} &= \nabla\cdot(-\sigma_{\rm io}\nabla\varphi_{\rm io}) \\ &= \begin{cases} -j_{\rm TPB}\lambda_{\rm TPB} & \text{in cathode} \\ 0 & \text{in electrolyte} \\ j_{\rm TPB}\lambda_{\rm TPB} & \text{in anode} \end{cases} \end{aligned} \tag{5}$$

$$j_{\rm TPB} = j_0\left[\exp\left(\frac{2\alpha_f F}{RT}\eta_{\rm act}\right) - \exp\left(-\frac{2\beta_f F}{RT}\eta_{\rm act}\right)\right] \tag{6}$$

For mass transport [20]:

$$\nabla N_i = \nabla\cdot(-D_i\nabla C_i + C_i\mathbf{u}) = R_i \tag{7}$$

$$\begin{aligned} N_i &= N_i^{\rm diffusioin} + N_i^{\rm convection} \\ &= -D_i\nabla C_i - C_i\frac{\bar{B}_2}{\mu}\nabla p \end{aligned} \tag{8}$$

$$\text{Anode}: \quad R_{\rm H_2} = -R_{\rm H_2O} = -\frac{i_{\rm el}}{2F} \tag{9}$$

$$\text{Cathode}: \quad R_{\rm O_2} = -\frac{i_{\rm el}}{4F} \tag{10}$$

$$\text{All others}: \quad R_i = 0 \tag{11}$$

For momentum transport:
(i) fuel channel,

$$\nabla\cdot\left\{\mu\left[\nabla\mathbf{u} + (\nabla\mathbf{u})^T\right]\right\} - \nabla p = \rho(\mathbf{u}\cdot\nabla)\mathbf{u} \tag{12}$$

(ii) porous electrode,

$$\begin{aligned} \frac{\mu}{B_0}\mathbf{u} &= -\nabla p + \nabla\cdot\left\{\frac{\mu}{\phi_{\rm g}}\left[\nabla\mathbf{u} + (\nabla\mathbf{u})^T\right]\right\} - \\ &\quad \nabla\cdot\left(\frac{2\mu}{3\phi_{\rm g}}\nabla\cdot\mathbf{u}I\right) \end{aligned} \tag{13}$$

DOI:10.1063/1674-0068/30/cjcp1704071

Most variables and parameters mentioned in Eq.(3)−Eq.(13) are self explanatory. Details about the governing equations and their source terms, boundary conditions, numerical grids and solver, basic parameters for physical properties of materials and cell operating conditions, *etc.*, are referred to Ref.[7]. The multiphysics model has been shown to provide *I-V* curves that are in very good agreement with the experimental results for both pSOFC and mtSOFC consisting of Ni-YSZ anode/YSZ electrolyte/LSM-YSZ cathode [7, 10, 21, 22].

Although the multiphysics model employs a set of governing equations that are quite general, the numerical results are dependent on the values of model parameters. To avoid using a large number of variable material parameters, only the material combination of Ni-YSZ anode/YSZ electrolyte/LSM-YSZ cathode with parameters described in Ref.[7] is considered here. Notice that this is not a limitation as it appears to be. Instead, the optimization results are in fact quite general. This is because that, as discussed above, the thicknesses of electrolyte and cathode are not the true geometric optimization targets. The optimal cell and electrolyte/cathode lengths are closely related to the electronic conductivity of the anode. Considering the fact that Ni is currently a universal material choice for SOFC anodes, the anode electronic conductivity is determined by the Ni content. Consequently, the Ni-YSZ based optimization results are of broad implications as they are valid also for other Ni based anode materials, *e.g.*, Ni-GDC, Ni-SDC, Ni-CGO, *etc.*

III. RESULTS AND DISCUSSION

A. Dependence of cell performance on the cathode location

The influence of the cathode location on the cell performance has been examined experimentally by comparing the electrochemical performances of four single cells [11]. The four single cells composed of Ni-YSZ anode/YSZ electrolyte/LSM-YSZ cathode were essentially identical, but differed in the distance, d, between the cathode and the anode current collector. The four single cells, cell A, cell B, cell C and cell D, correspond to d=2, 5, 8 and 14 cm, respectively. Geometric models were built to correspond to the specifications of the four single cells and the same set of property parameters as described in Ref.[7] was applied for the multiphysics simulations. The parameter set of Ref.[7] have been shown to reproduce the experimental results of Ref.[10] very well. With this set of parameters, the theoretical *I-V* curves for the four single cells are shown together with the experimental data in FIG. 2. As seen in FIG. 2, the theoretical and experimental results are in very good agreement. The result is remarkable as the values of all the model parameters are exactly the same as that in Ref.[7] and there is no fitting parameter used in this study. The ability to reproduce two independent experiments [10, 11] with the same set of parameters demonstrates convincingly the predictive power of the multiphysics model employed here.

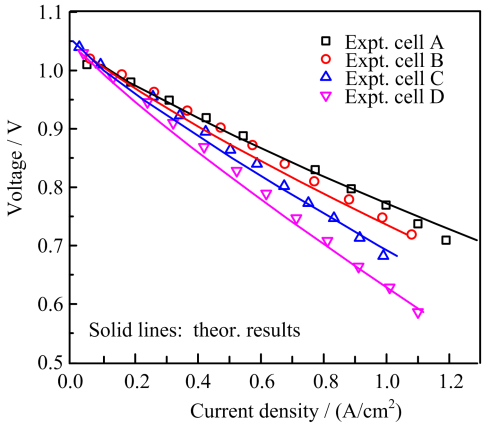

FIG. 2 Comparison of the theoretical and experimental *I-V* curves of four single cells A, B, C, D that differ in the distance d between the cathode and the anode current collector with d=2, 5, 8, 14 cm, respectively.

The decreased cell performance with the increased d shown in FIG. 2 is simply due to the associated increase of the ohmic loss of current collection. The current is collected by traveling a distance of d and passing through a cross section area:

$$\begin{aligned} A_{\rm an} &= \pi[(r_{\rm in}+t_{\rm an})^2 - r_{\rm in}^2] \\ &= \pi t_{\rm an}(2r_{\rm in}+t_{\rm an}) \end{aligned} \tag{14}$$

For the above four single cells, $t_{\rm an}\approx r_{\rm in}\approx$1.5 mm [11] and $A_{\rm an}$ is relatively large at about 20 mm^2. For such a large $A_{\rm an}$, the decrease in the cell performance is already noticeable for a distance of a few centimeters, as shown in FIG. 2. For a typical mtSOFC with $A_{\rm an}\approx$1 mm^2 [4], a cell performance decrease is therefore expected to be substantial for an increase of d in the order of a few millimeters. As a result, the benefit of increasing $l_{\rm ca}$ for the cell current production quickly diminishes while the rate of cell volume increase remains constant. Therefore, finding an optimal $l_{\rm ca}$ that maximizes VPD is important in practice.

B. Optimal cell length with single-terminal anode current collection

Multiphysics simulations were performed for 20 combinations of ($r_{\rm in}$, $t_{\rm an}$), with $r_{\rm in}$=(0.4, 0.85, 1.5, 3.0, 5.0 mm) and $t_{\rm an}$=(100, 200, 300, 500 μm). The ranges of $r_{\rm in}$ and $t_{\rm an}$ are chosen to cover the ranges of tube radius and anode thickness of known mtSOFCs that use anode tube terminal current collection [4]. $l_{\rm ca}$ is varied for the search of MVPD. The optimal $l_{\rm ca}$ and the corresponding MVPD for each of the 20 combinations of ($r_{\rm in}$, $t_{\rm an}$) are shown in Table I.

DOI:10.1063/1674-0068/30/cjcp1704071

TABLE I Cell lengths that maximize VPD at T=1073.15 K for different combinations of anode thickness, t_{an}, and inner tube radius, r_{in}. The cell uses a single-terminal anode current collector and l_{cell}=l_{ca}+6 mm. l_{ca} is in mm and MVPD in W/cm^3.

r_{in}/mm	t_{an}=100 μm		t_{an}=200 μm		t_{an}=300 μm		t_{an}=500 μm		Optimal
	l_{ca}	MVPD	l_{ca}	MVPD	l_{ca}	MVPD	l_{ca}	MVPD	(t_{an}, l_{ca}, MPVD)
0.4	5.95	18.9	7.18	17.8	8.08	16.0	9.26	12.9	(85, 5.78, 19.1)
0.85	6.13	10.5	7.54	10.7	8.46	10.4	9.90	9.31	(190, 7.40, 10.7)
1.5	6.30	6.34	7.72	6.80	8.70	6.80	10.2	6.49	(248, 8.19, 6.86)
3.0	6.34	3.32	7.84	3.67	8.82	3.81	10.4	3.80	(396, 9.56, 3.85)
5.0	6.35	2.03	7.90	2.27	8.90	2.38	10.4	2.44	(567, 10.8, 2.44)

As seen in Table I, the optimal cell length, or the corresponding l_{ca}, is mainly determined by t_{an} and weakly dependent on r_{in}. On one hand, as can be seen in Eq.(2) and Eq.(14), for a given r_{in}, an increase of t_{an}, Δt_{an}, causes a relative increase of A_{an} by

$$\frac{\Delta A_{an}}{A_{an}} = \frac{\Delta t_{an}}{t_{an}} \frac{r_{in} + t_{an} + \Delta t_{an}/2}{r_{in} + t_{an}/2} > \frac{\Delta t_{an}}{t_{an}} \tag{15}$$

and a relative increase of A_{EC} by

$$\frac{\Delta A_{EC}}{A_{EC}} = \frac{\Delta t_{an}}{r_{in} + t_{an}} < \frac{\Delta t_{an}}{t_{an}} \tag{16}$$

Due to the extra capacity of current conduction provided by the larger increase of A_{an}, l_{ca} increases with t_{an}, as shown in Table I. On the other hand, for a given t_{an}, an increase of r_{in}, Δr_{in}, corresponds to

$$\frac{\Delta A_{an}}{A_{an}} = \frac{\Delta r_{in}}{r_{in} + t_{an}/2} \tag{17}$$

$$\frac{\Delta A_{EC}}{A_{EC}} = \frac{\Delta r_{in}}{r_{in} + t_{an}} \tag{18}$$

That is, $\Delta A_{an}/A_{an}$ is only slightly larger than $\Delta A_{EC}/A_{EC}$. As a result, there is only a small increase of l_{ca} for the increase of r_{in}.

The optimal t_{an} for a given r_{in}, in terms of yielding the highest MVPD, is also shown together with the optimized l_{ca} and MVPD in Table I. As expected and discussed above, Table I shows that MVPD increases with the reduced r_{in}. A small r_{in} means a small A_{EC} and does not require a large current conducting capacity. Meanwhile, an increase of t_{an} corresponds to a large relative change in V_{cell}. As a result, the optimal t_{an} for finding MVPD is small for a small r_{in}, as seen in Table I.

It should be noticed that the data in Table I are obtained with a set of conventional and mature materials, *i.e.*, Ni-YSZ anode/YSZ electrolyte/LSM-YSZ cathode. A thickness of 5 μm assumed for the electrolyte layer should also impose no significant challenge on fabrication technique [4, 17, 18]. The tube outer diameter for practical mtSOFCs is often under 2 mm [4]. Such a tube is about the size of the tube with r_{in}=850 μm and t_{an}=150−200 μm. Moreover, an ample room, Δl=6 mm of the tube length, has been allocated for the current collection and stack assembly [23]. Therefore, it may be concluded that the seemingly high MVPD=11 W/cm^3 for r_{in}=0.85 mm is not only achievable, but also surpassable in practice.

As the practical l_{ca} may not be optimal due to various considerations, FIG. 3 shows the dependence of the maximum area specific power density, p_m=P_m/A_{EC}, on l_{ca} for three combinations of (r_{in}, t_{an}): (0.4 mm, 100 μm), (0.85 mm, 200 μm), (1.5 mm, 300 μm). The three (r_{in}, t_{an}) combinations are representative as r_{in}∈(0.4 mm, 1.5 mm) and t_{an}∈(100 μm, 300 μm) are reported for most mtSOFCs [4]. For other practically chosen (r_{in}, t_{an}) with r_{in} and t_{an} in the above stated range, p_m may be estimated by suitable interpolation. Together with Δl required in practice, VPD can then be predicted and used to help the design of mtSOFC. As a special case of practical interest, FIG. 3 shows that p_m≈0.9 W/cm^2 may be expected for as-mtSOFC with (r_{in}=0.85 mm, t_{an}=200 μm, l_{ca}=10 mm).

C. Optimal cell length with double-terminal anode current collection

Similar to the cases with single-terminal anode current collection (STACC), multiphysics simulations were performed for mtSOFCs with double-terminal anode current collection (DTACC). The results for the optimal l_{ca} and MVPD are shown in Table II. Due to the same reason analyzed above, the results shown in Table II and Table I are qualitatively the same concerning: (i) l_{ca} increases with the increase of t_{an} much more than with the increase of r_{in}. (ii) MVPD decreases while the optimal t_{an} increases with the increase of r_{in}. Moreover, it is natural to see that l_{ca} and MVPD are larger for DTACC than for STACC. Though the length of current pathway is cut by half from STACC to DTACC, l_{ca}(DTACC) is less than 2l_{ca}(STACC) for MVPD as p_m decreases with l_{ca}, as shown in FIG. 3. As a result, l_{ca}(DTACC) is about 60% larger than l_{ca}(STACC) for finding MVPD. It is noted in Table I that l_{ca}(DTACC)/l_{ca}(STACC) is fairly constant, whereas MVPD(DTACC)/MVPD(STACC) shows a little more variation and decreases with the increased l_{ca}. Nevertheless, it is a good approximations to say that MVPD(DTACC) is 30% higher

DOI:10.1063/1674-0068/30/cjcp1704071

TABLE II Cell lengths that maximize VPD at T=1073.15 K for different combinations of (r_{in}, t_{an}). The cell uses a double-terminal anode current collector and $l_{cell}=l_{ca}+6$ mm. l_{ca} is in mm and MVPD in W/cm^3.

r_{in}/mm	t_{an}=100 μm		t_{an}=200 μm		t_{an}=300 μm		t_{an}=500 μm		Optimal
	l_{ca}	MVPD	l_{ca}	MVPD	l_{ca}	MVPD	l_{ca}	MVPD	(t_{an}, l_{ca}, MPVD)
0.4	9.44	25.8	11.6	23.4	12.9	20.8	14.9	16.6	(81, 8.91, 26.0)
0.85	9.77	15.2	12.0	14.0	13.6	13.3	15.7	11.7	(140, 10.7, 16.1)
1.5	9.90	8.55	12.3	8.83	13.9	8.69	16.2	8.11	(216, 12.5, 8.83)
3.0	9.99	4.47	12.3	4.78	14.1	4.83	16.5	4.72	(323, 14.4, 4.83)
5.0	10.0	2.71	12.4	2.92	14.1	3.00	16.5	3.01	(442, 15.8, 3.02)

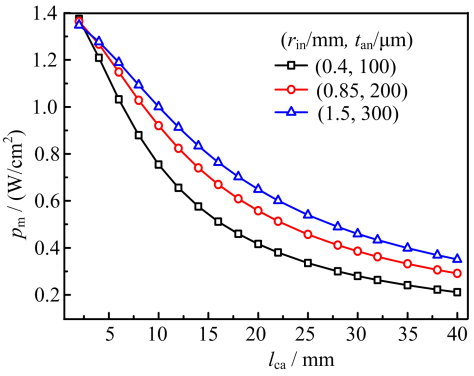

FIG. 3 The maximum area specific power density, p_m, by single-terminal anode current collection (STACC) *vs.* the cathode length, l_{ca}, for (r_{in}, t_{an})=(0.4 mm, 100 μm), (0.85 mm, 200 μm) and (1.5 mm, 300 μm).

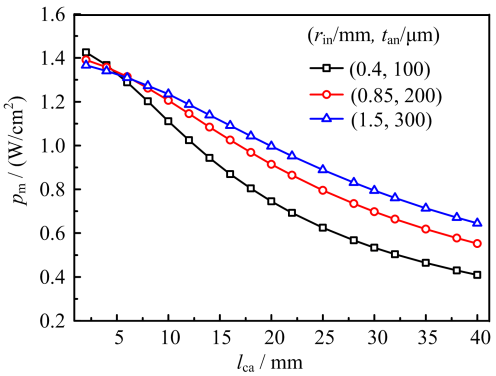

FIG. 4 p_m by double-terminal anode current collection (DTACC) *vs.* l_{ca} for (r_{in}, t_{an})=(0.4 mm, 100 μm), (0.85 mm, 200 μm) and (1.5 mm, 300 μm).

than MVPD(STACC). For the practical combination of (r_{in}≈0.85 mm, t_{an}≈150 μm), an MVPD of over 15 W/cm^3 may be expected with DTACC.

To provide more information about the performance of mtSOFC versus the tube size, FIG. 4 shows the dependence of p_m on l_{ca} for the three combinations of (r_{in}, t_{an}): (0.4 mm, 100 μm), (0.85 mm, 200 μm), (1.5 mm, 300 μm). Comparison of FIG. 3 and 4 shows clearly that p_m is higher for DTACC than for STACC. Notice that theoretically p_m for DTACC is the same as p_m for STACC when l_{ca} approaches zero. The improvement on p_m with DTACC is attributed to the fact that the length of current conducting path and the amount of current collected by each collector are both cut by half in comparison with that in STACC. The ohmic loss with DTACC is reduced by the shortened conducting path and the reduced current amount. As both the conducting path and the total current increase with l_{ca}, the ohmic loss reduction increases with the increased l_{ca}. Consequently, the improvement on p_m with DTACC increases with the increased l_{ca}. Similarly, p_m with DTACC deceases slower than that with STACC for the increased l_{ca}, as shown in FIG. 3 and 4. Increasing l_{ca} for the increased p_m is more meaningful with DTACC than with STACC. Though STACC may be convenient and is the main method in use, the effort of developing DTACC technique is worthwhile for reasonably large l_{ca}, say, 6 mm or more. For (r_{in}=0.85 mm, t_{an}=200 μm, l_{ca}=10 mm), p_m is increased from 0.9 W/cm^2 for STACC to 1.2 W/cm^2 for DTACC.

D. Primitive comparison of the performances of mtSOFC and pSOFC

It is a common perception that mtSOFC is advantageous on thermal shock resistance and fast startup as well as thermal cycling, but suffers from the drawback of much lower current output than that of pSOFC. As shown above, however, the cell current production can be substantially improved by the geometric optimization and by using DTACC instead of the conventional STACC. In fact, FIG. 4 indicates that the performance of mtSOFC can be comparable with that of the state of the art pSOFC [21]. It should be interesting to compare the performances of mtSOFC and pSOFC. However, a quality comparison should examine the effect of a number of key design parameters and require a dedicated effort of study. Consequently, only a preliminary comparison is made here.

As the experimental results reported in Ref.[21] are representative of the best performing pSOFC, the same set of materials and relevant geometric parameters are used for mtSOFC. In addition, the practical parameters

DOI:10.1063/1674-0068/30/cjcp1704071

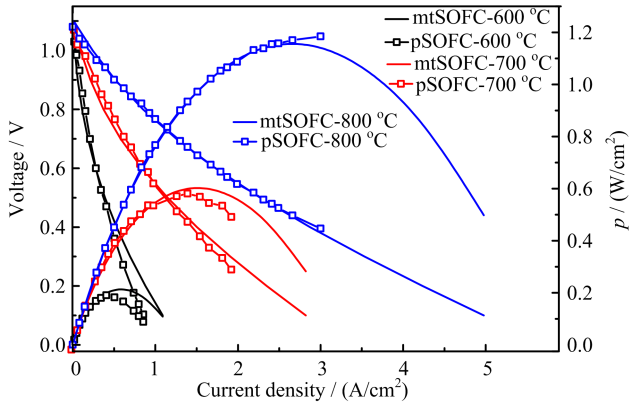

FIG. 5 Comparison of I-V and I-p relations of mtSOFC and pSOFC (p: area specific power density).

of ($r_{\rm in}$=0.85 mm, $t_{\rm an}$=200 μm, $l_{\rm ca}$=10 mm) are assigned for the mtSOFC. FIG. 5 compares the I-V curves and power densities of the theoretical mtSOFC and experimental pSOFC cells.

As shown in FIG. 5, the power output of mtSOFC is in fact quite comparable to its pSOFC counterpart. This is understandable as the material properties of the two cells are similar and the extra ohmic loss in mtSOFC with $l_{\rm ca}$=10 mm and $t_{\rm an}$=200 μm is quite limited (FIG. 4). That is, with proper selections of geometric parameters, the electrochemical performance of mtSOFCs can be sufficiently high and very close to that of pSOFCs. The observed phenomenon that the current output of mtSOFC is much lower than that of pSOFC is caused by immature fabrication technique and poor choice of geometric parameters. In other words, the common perception that the current output of mtSOFC is much lower than that of pSOFC is inaccurate and misguided.

IV. CONCLUSION

Based on this study, the following results are obtained. (i) $r_{\rm in}$, $t_{\rm an}$ and $l_{\rm ca}$ are the main geometric parameters affecting VPD of as-mtSOFC. (ii) The multiphysics model employed is capable of reproducing experimental I-V curves with no adjustable parameters. (iii) The optimal values of $l_{\rm ca}$ and the corresponding MVPDs are found for 20 combinations of ($r_{\rm in}$, $t_{\rm an}$) with five representative $r_{\rm in}$ and four representative $t_{\rm an}$. (iv) The variation of $p_{\rm m}$ with $l_{\rm ca}\in$(2 mm, 40 mm) is determined for three representative combinations of ($r_{\rm in}$, $t_{\rm an}$). (v) The electrochemical performances of mtSOFC and pSOFC are comparable.

The numerical results show that: (i) for ($r_{\rm in}$=850 μm, $t_{\rm an}$=200 μm) representative of the practical as-mtSOFCs and T =800 °C, the seemingly high MVPD of 11 and 14 W/cm^3 can be easily realized for STACC and DTACC, respectively; (ii) considering the practical $l_{\rm ca}$ of about 1 cm, it is realistic to expect $p_{\rm m}$ of about 0.9 and 1.2 W/cm^2 for as-mtSOFC with STACC and DTACC, respectively; (iii) significant performance improvement may be achieved by geometry optimization. The performance of optimized as-mtSOFC is comparable to that of pSOFC. Based on these numerical results, it is concluded that mtSOFC is a promising technology for vehicle applications.

V. ACKNOWLEDGMENTS

This work was supported by the National Natural Science Foundation of China (No.11374272 and No.11574284) and the Collaborative Innovation Center of Suzhou Nano Science and Technology.

[1] T. Suzuki, Z. Hasan, Y. Funahashi, T. Yamaguchi, Y. Fujishiro, and M. Awano, Science **325**, 852 (2009).
[2] K. K. T. Alston, M. Palin, M. Prica, and P. Windibank, J. Power Sources **71**, 271 (1998).
[3] V. Lawlor, S. Griesser, G. Buchinger, A. G. Olabi, S. Cordiner, and D. Meissner, J. Power Sources **193**, 387 (2009).
[4] V. Lawlor, J. Power Sources **240**, 421 (2013).
[5] J. Li and Z. Lin, Int. J. Hydrogen Energ. **37**, 12925 (2012).
[6] A. Li, C. Song, and Z. Lin, Appl. Energ. **190**, 1234 (2017).
[7] J. Li, W. Kong, and Z. Lin, J. Power Sources **232**, 106 (2013).
[8] B. X. Wang, Z. Jiang, and Z. J. Lin, Chin. J. Chem. Phys. **28**, 299 (2015).
[9] K. S. Howe, G. J. Thompson, and K. Kendall, J. Power Sources **196**, 1677 (2011).
[10] C. Yang, W. Li, S. Zhang, L. Bi, R. Peng, C. Chen, and W. Liu, J. Power Sources **187**, 90 (2009).
[11] C. Jin, J. Liu, L. Li, and Y. Bai, J. Membrane Sci. **341**, 233 (2009).
[12] T. Suzuki, Y. Funahashi, T. Yamaguchi, Y. Fujishiro, and M. Awano, Solid State Ionics **180**, 546 (2009).
[13] A. Mirahmadi and K. Valefi, Ionics **17**, 767 (2011).
[14] Y. Funahashi, T. Shimamori, T. Suzuki, Y. Fujishiro, and M. Awano, J. Power Sources **163**, 731 (2007).
[15] A. Li and Z. Lin, Chin. J. Chem. Phys. **30**, 139 (2017).
[16] S. B. Lee, K. i. S. Yun, T. H. Lim, R. H. Song, and D. R. Shin, ECS Transactions **7**, 187 (2007).
[17] T. Suzuki, M. H. Zahir, T. Yamaguchi, Y. Fujishiro, M. Awano, and N. Sammes, J. Power Sources **195**, 7825 (2010).
[18] S. Lee, T. Lim, R. Song, D. Shin, and S. Dong, Int. J. Hydrogen Energ. **33**, 2330 (2008).
[19] D. Chen, W. Bi, W. Kong, and Z. Lin, J. Power Sources **195**, 6598 (2010).
[20] W. Kong, H. Zhu, Z. Fei, and Z. Lin, J. Power Sources **206**, 171 (2012).
[21] F. Zhao and A. Virkar, J. Power Sources **141**, 79 (2005).
[22] W. Kong, J. Li, S. Liu, and Z. Lin, J. Power Sources **204**, 106 (2012).
[23] N. M. Sammes, Y. Du, and R. Bove, J. Power Sources **145**, 428 (2005).

DOI:10.1063/1674-0068/30/cjcp1704071